UNIVERSITY OF THESSALY
SCHOOL OF ENGINEERING
DEPARTMENT OF MECHANICAL ENGINEERING

FINITE ELEMENT SIMULATION OF ROLLING MANUFACTURING PROCESS FOR COLD-FORMED STEEL MEMBERS

By
NIKOLAOS PANTEKIS

Submitted in partial fulfillment of the requirements for the degree of Diploma in Mechanical Engineering at the University of Thessaly

Volos, 2024

UNIVERSITY OF THESSALY
SCHOOL OF ENGINEERING
DEPARTMENT OF MECHANICAL ENGINEERING

FINITE ELEMENT SIMULATION OF ROLLING MANUFACTURING PROCESS FOR COLD-FORMED STEEL MEMBERS

By
NIKOLAOS PANTEKIS

Submitted in partial fulfillment of the requirements for the degree of Diploma in Mechanical Engineering at the University of Thessaly

Volos, 2024

Approved by the Committee on Final Examination:

Advisor Dr. Spyros Karamanos,
Professor, Department of Mechanical Engineering,
University of Thessaly

Member Dr. Alexis Kermanidis,
Associate professor, Department of Mechanical Engineering,
University of Thessaly

Member Dr. Emmanouil Bouzakis,
Associate professor, Department of Mechanical Engineering,
University of Thessaly

Date Approved: [March 11, 2024]

FINITE ELEMENT SIMULATION OF ROLLING MANUFACTURING PROCESS FOR COLD-FORMED STEEL MEMBERS

PANTEKIS NIKOLAOS

Department of Mechanical Engineering, University of Thessaly

Supervisor: Spyros A. Karamanos, Ph.D.

Professor, Department of Mechanical Engineering, University of Thessaly

Abstract

Cold roll-formed steel sections find extensive use in the construction of warehouses. The sheet metal utilized in crafting these components is stored and transported in the form of metal coils for compactness and ease of transport. The metal sheets undergo bending during coiling and uncoiling before undergoing further shaping through the rollers. Examining the impact this process can have on the extent of plastic deformation and the final cross-sectional dimensions of such components is valuable. Predictive models exist that are designed to account for these factors. Their objective is to characterize material enhancements, resulting in structural sections with properties surpassing their nominal values. Notably in the corners of the sections, deformations caused by the forming process alter the material's behavior. The yield strength is expected to increase, leading to reduced ductility and the formation of residual stresses. The final section exhibits the ability to withstand greater loads and resist buckling more effectively. While these structural strength enhancements can be verified with experimental testing, this study aims to affirm these results through finite element analysis and focuses on the cold roll-forming process of section P140/120/3.5 with S355MC material, a mild grade steel intended for applications where high strength is paramount. A simulation model developed by Christos Prosgolitis, Spyros Karamanos, and Alexis Kermanidis at the University of Thessaly within the laboratories of the Department of Mechanical Engineering, employing the finite element analysis software ABAQUS/Implicit, is utilized in this study. Several methods to complete this simulation in a reduced time are tested and a bending simulation is created which simulates the sheet metal coiling and uncoiling. The plate is then subjected to roll-forming and material is analyzed with a uniaxial tensile test simulation. A substantial increase in yield strength is observed in the flat regions while the corners display only marginal improvement.

Key words: roll-forming, cyclic loading, coil, sheet, shell, springback, hardening, enhancements, yield, finite element analysis

ΠΡΟΣΟΜΟΙΩΣΗ ΠΕΠΕΡΑΣΜΕΝΩΝ ΣΤΟΙΧΕΙΩΝ ΤΗΣ ΚΑΤΕΡΓΑΣΙΑΣ ΔΙΑΜΟΡΦΩΣΗΣ ΧΑΛΥΒΔΙΝΩΝ ΕΛΑΣΜΑΤΩΝ ΜΕΣΩ ΨΥΧΡΗΣ ΕΛΑΣΗΣ

ΠΑΝΤΕΚΗΣ ΝΙΚΟΛΑΟΣ

Τμήμα Μηχανολόγων Μηχανικών, Πανεπιστήμιο Θεσσαλίας

Επιβλέπων Καθηγητής: Δρ. Σπύρος Καραμάνος,

Καθηγητής, Τμήμα Μηχανολόγων Μηχανικών, Πανεπιστήμιο Θεσσαλίας

Περίληψη

Οι χαλύβδινες διατομές που διαμορφώνονται με ψυχρή έλαση βρίσκουν εκτεταμένη χρήση στην κατασκευή αποθηκών. Τα ελάσματα που χρησιμοποιούνται για την κατασκευή τους αποθηκεύονται και μεταφέρονται με τη μορφή μεταλλικών σπειρών λόγω όγκου και ευκολίας μεταφοράς. Τα ελάσματα υφίστανται κάμψη κατά την περιέλιξη και το ξετύλιγμα τους και έπειτα υπόκεινται σε περαιτέρω διαμόρφωση μέσω των ράουλων έλασης. Η εξέταση των επιπτώσεων που μπορεί να έχει αυτή η διαδικασία στο μέγεθος της πλαστικής παραμόρφωσης και στις τελικές διαστάσεις τέτοιων διατομών είναι πολύτιμη. Υπάρχουν προγνωστικά μοντέλα που έχουν σχεδιαστεί για να λάβουν υπόψη αυτούς τους παράγοντες. Στόχος τους είναι να χαρακτηρίσουν τις βελτιώσεις των υλικών που έχουν ως αποτέλεσμα μεταλλικές διατομές με ιδιότητες που ξεπερνούν τις ονομαστικές τους. Ιδιαίτερα στις γωνίες αυτών, οι παραμορφώσεις που προκαλούνται από τη διαδικασία διαμόρφωσης αλλάζουν τη συμπεριφορά του υλικού. Η αντοχή στην διαρροή αναμένεται να αυξηθεί οδηγόντας στην μείωση της ολκιμότητας και τον σχηματισμό παραμενόντων τάσεων. Οι τελικές διατομές παρουσιάζουν την ικανότητα να αντέχουν μεγαλύτερα φορτία και να αντιστέκονται στον λυγισμό πιο αποτελεσματικά. Αν και αυτές οι βελτιώσεις μπορούν να επαληθευτούν με πειραματικές δοκιμές, αυτή η μελέτη στοχεύει να επιβεβαιώσει αυτά τα αποτελέσματα μέσω ανάλυσης πεπερασμένων στοιχείων. Εστιάζει στη διαδικασία διαμόρφωσης ψυχρής έλασης της διατομής P140/120/3.5 με υλικό S355MC, έναν μαλακό χάλυβα που προορίζεται για εφαρμογές όπου η υψηλή αντοχή είναι πρωτεύουσας σημασίας. Γίνεται η χρήση ενός μοντέλου προσομοίωσης που αναπτύχθηκε από τους: Χρήστο Προσγολίτη, Σπύρο Καραμάνο και Αλέξη Κερμανίδη στο Πανεπιστήμιο

Θεσσαλίας, στα εργαστήρια του Τμήματος Μηχανολόγων Μηχανικών, χρησιμοποιώντας το λογισμικό ανάλυσης πεπερασμένων στοιχείων ABAQUS/Implicit. Εξετάζονται διάφορες μέθοδοι για την ολοκλήρωση αυτής της προσομοίωσης σε μειωμένο χρόνο και δημιουργείται μια προσομοίωση κάμψης που προσομοιώνει την περιέλιξη και το ξετύλιγμα του ελάσματος, το οποίο στη συνέχεια υποβάλλεται σε μορφοποίηση μέσω ράουλων έλασης. Έπειτα το υλικό αναλύεται με χρήση μιας προσομοίωσης μονοαξονικού εφελκυσμού. Σημαντική βελτίωση της αντοχής σε διαρροή παρατηρείται στις επίπεδες περιοχές ενώ οι γωνίες εμφανίζουν μόνο οριακή αύξηση.

Λέξεις-κλειδιά: ψυχρή έλαση, κυκλική καταπόνηση, σπείρα, συσπείρωση, έλασμα, στοιχεία κελύφους, ελαστική επαναφορά, σκλήρυνση, όριο διαρροής

Contents

LIST OF FIGURES

LIST OF TABLES

Chapter 1 INTRODUCTION AND LITERATURE REVIEW

1.1 Motivation

In the scope of the European project “FAtigue STrength of COLD-formed structural steel details” (FASTCOLD) [1], a study on the resulting local residual stresses of a cold roll-forming process of an omega shaped profile was performed by Christos Prosgolitis, Spyros Karamanos and Alexis Kermanidis at the University of Thessaly at the Department of Mechanical Engineering. Factors such as number of roll forming stations and their distance, contact and element type and their impact on work hardening and final geometry were identified as deserving further research. Furthermore, there was an interest in integrating a more complete history for the material of the metal plate that undergoes roll-forming. This involves investigating the impact of plate coiling and uncoiling on the extent of work hardening.

1.2 Introduction To Literature Review

In roll-forming, metal sheets undergo progressive deformation as they travel through each forming station that bends the material to match the rollers radius and shape. The strip is guided through the rollers with frictional forces with an objective of creating the desired bends in the material without causing major defects in both the cross-sectional and longitudinal directions. The thickness of the sheet should not change significantly during the bending process, crucial for achieving the desired mechanical properties and tolerances in the final product. Phenomena such as springback, buckling of the flat faces, and material hardening or softening are considered. With the right roller design, it becomes possible to shape sections with significant intricacy. Ultimately, the result of the bending process is the section's final shape which exhibits significant residual stresses in the folding regions.

Given that these regions can constitute a substantial portion of the section, it has been supported for their structural effect to be considered in the sections final properties [2,3]. Corner strength enhancement can depend on a lot of factors such as material properties, load history, deformation rate and corner radius to thickness ratio. Thinner gauge steel is most notably cold-rolled at ambient temperatures and is subjected to plastic deformations both during its manufacturing steps and the roll-forming process. Therefore the effects of sheet metal coiling and uncoiling should be considered for material properties [4,5]. On this basis, predictive models attempt to combine experimental data to formulate changes in material yield strength.

Computational modeling is also combined in pursuit of such characteristics and for a better understanding of the ultimate load bearing capacities of these sections [6]. Analysing them with the use of finite element analysis can be both complicated and straightforward as it necessitates careful choice of parameters and model setup through an understanding of their capabilities and limitations [7]. Small differences in selection can lead to bigger than expected changes and the results should therefore be eventually validated with experimental data.

Based of these fundamentals, deformations caused by sheet metal manufacturing and transport in combination with residual stresses, strain hardening and cyclic phenomena that occur during the roll-forming process have to be considered for accurate description of the strength properties of formed sections.

1.3 Diploma Thesis Organization

This thesis is structured into three main sections. In the first part, the focus is placed on reducing the simulation time which approximately requires three days. Various approaches are explored to achieve this goal, including replacing three-dimensional elements with shell elements, decreasing the number of roll-forming stations, and dividing the simulation into segments. Upon careful consideration, the second approach is selected for further progression. The second part of the thesis is dedicated to establishing suitable hardening parameters with the help of experimental hysterisis loop data and subsequently performing a bending simulation using these parameters. Finally, the strain-hardened plate is subjected to roll-forming, and comprehensive data analysis is conducted on different sections of the plate.

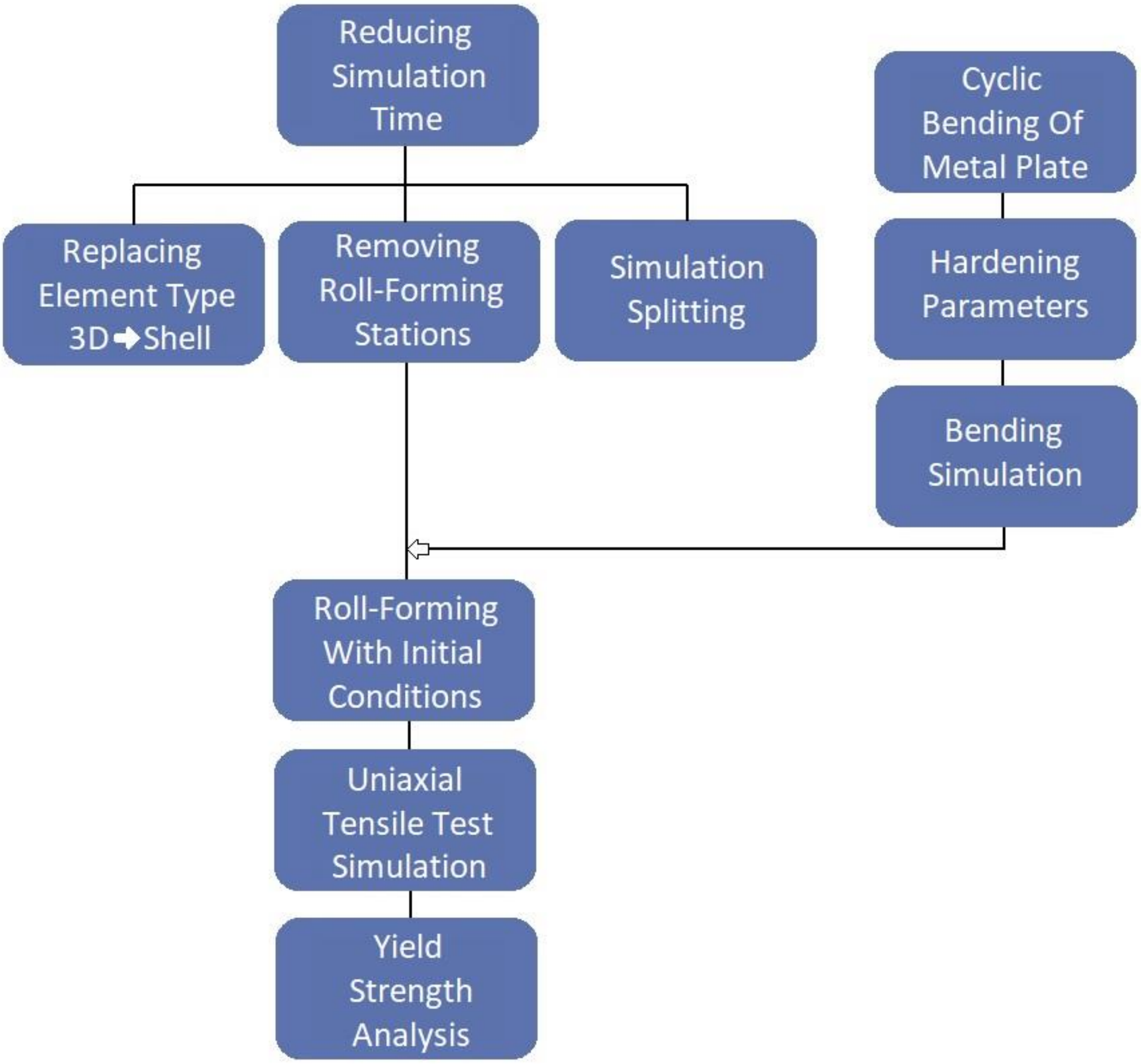

Figure: 1.2.1: Overview of diploma thesis

Chapter 2 REDUCING SIMULATION TIME

2.1 ABAQUS Model Overview

The flower pattern of the P140/120/3.5 profile (Figure 2.1.1) consists of five corners and is formed over 28 stations. The simulated sheet metal plate has dimensions of 650 mm in length, 220 mm in width, and 3 mm in thickness. Initially twice the length was used to ensure that at least two roller stations are actively involved in the forming process at all times as the plate advances to the next station. Using a plate of half the length would result in contact with only one station for a significant part of its travel. While this approach overlooks certain factors influencing the final shape and residual stresses of the plate and is less faithfull to a real life scenario, this compromise is accepted as the computational load of the simulation is significantly reduced when the plate's length is halved.

Material tests performed by Christos Prosgolitis at the University of Thessaly within the laboratories of the Mechanical Engineering Department yield experimental stress-strain data. These are input as a dataset into ABAQUS and are transformed into true values using the calibration function. This results in a linear hardening model utilizing a specific number of points, referred to as plastic points, to approximate the stress-strain curve, establishing an elastic-plastic isotropic behavior for the material. The plate is defined as a solid deformable component with a Young's modulus of elasticity of 200 GPa and a Poisson's ratio of 0.3.

The chosen element type is C3D8R with a length of 40 mm, a width of 4 mm which gradually decreases to 0.5 mm in five folding regions and a thickness of 0.7 mm which results in five elements across the thickness. The material behavior is isotropic elastic and isotropic plastic. The rollers are defined as analytical rigid components, and the interaction between the plate and the rollers involves frictionless tangential behavior with hard contact in the normal direction. This interaction utilizes surface-to-surface contact with node-to-surface discretization. Due to symmetry in the rolling direction, only half of the plate is modeled.

To guide the plate through the rollers, a displacement-based boundary condition is applied to the plate. The rollers remain stationary, resulting in a static shaping of the plate, as opposed to a dynamic simulation in which the plate's movement is driven by roller rotation and friction. Existing literature suggests that both static and dynamic predictions produce nearly indistinguishable outcomes, with the former being much more efficient regarding computation time [8].

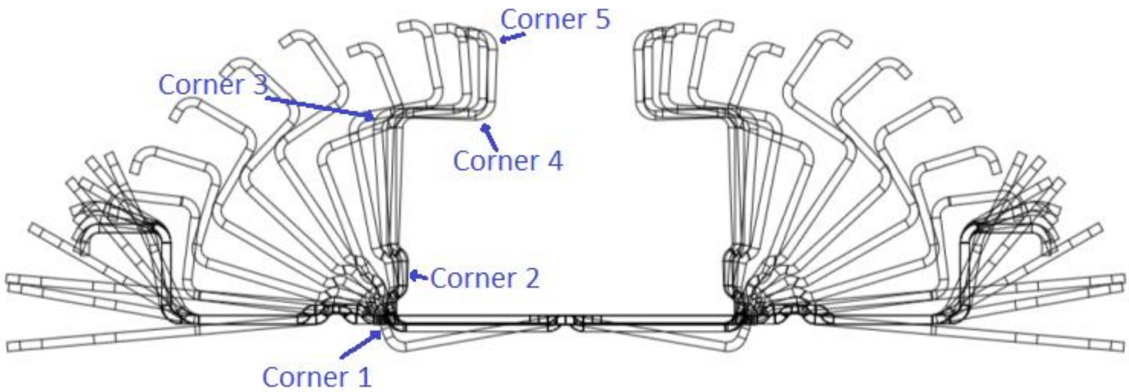

Figure 2.1.1: Flower pattern profile [1]

Upon successfully completing the simulation, several observations were made. Firstly, an apparent error in the final geometry of one of the rollers, specifically the top roller of station 22, which forms a curve to shape the corner at the location of symmetry (Figure 2.1.1). While the sketch and resulting geometry in the ABAQUS assembly are correct, there is an inaccuracy in the simulated result (Figure 2.1.2). As the geometries were designed in a different computer-aided design software and then imported into ABAQUS, it is possible that some artifacts or discontinuities in the sketch were introduced as a result. This issue can be easily rectified by deleting that part of the geometry, resketching it with the same dimensions, and saving the changes.

Secondly, distortion is observed in the profiles' shape due to interference between the plate and the rollers as it passes through and is progressively bent. The source of this interference can be traced back to stations 18 and 19 (Figure 2.1.3). The issues begin once the plate enters station 19 and is pushed onto the top roller of the station prior. To address this problem, reducing the size of the top roller in station 18 has proven to be effective. This adjustment allows the roller to fit smoothly under the bend of corner 3 and eliminates the interference. This distortion cannot be attributed to the reduced length of the plate, as correcting it requires modifications to roller geometry, station distance, or the addition of another roll-forming station to facilitate a more gradual bending process. Even if the plate's length is doubled, mitigating this undesired deformation would still rely on the same adjustments.

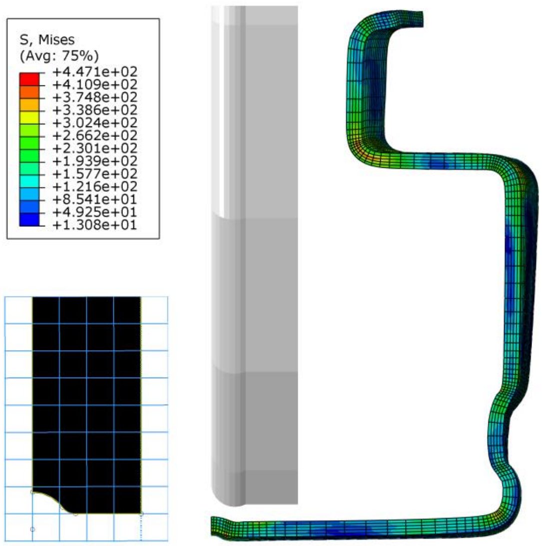

Figure 2.1.2: Sketch of top roller 22 in black with incorrect geometry in grey; final shape of section with visible defect caused by interference

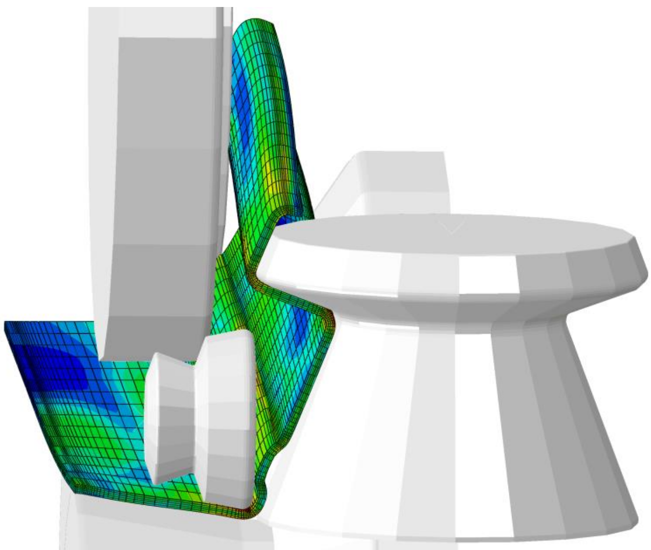

Figure 2.1.3: Interference between top roller of station 18 (in the back) and metal plate

2.2 Replacing Three Dimensional Elements With Shell Elements

One of the main objectives of this study is to employ shell elements instead of three-dimensional elements. Their utilization offers several advantages, particularly when addressing nonlinear material behavior and handling large deformations.

The recreated shell plate maintains the same mesh size with only one element across its thickness (Figure 2.2.1). This shell plate necessitates surface-to-surface rather than node-to-surface discretization, as the thickness must be considered since node based surfaces do not have thickness. Finite sliding is preferred over the small sliding formulation, as the latter is not suitable for the expected contact conditions. A state-based tracking algorithm is selected as it is the only available tracking method for finite sliding, surface-to-surface contact involving analytical rigid surfaces.

Analytical rigid parts are automatically designated as the master surfaces of contact, making the shell plate the slave surface. This type of contact requires more computational power since it involves a greater number of nodes for each constraint [9]. Particularly when the model experiences contact over a large portion of its area, the cost of the solution is increased. Nonetheless, considering that the total number of iterations required for convergence can be smaller even though each iteration is more computationally intensive, it is not always clear in advance which type of contact offers superior efficiency.

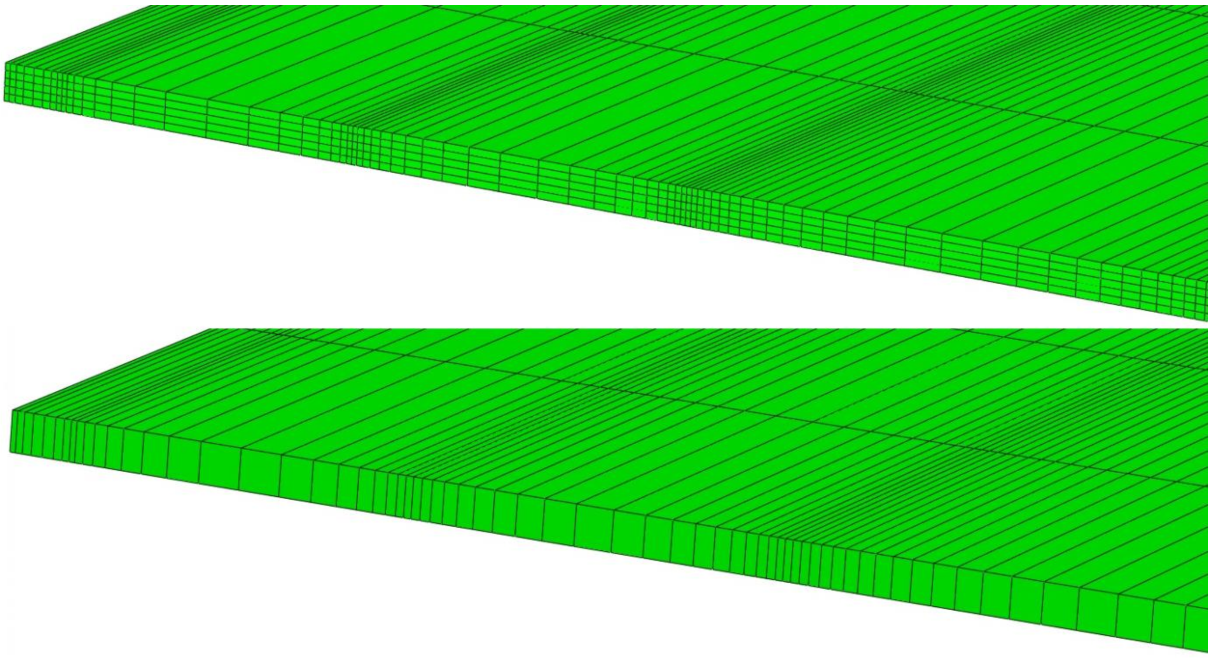

Figure 2.2.1: 3D and shell element plate

The plate has been assigned a homogeneous shell section rather than a solid one, with a shell thickness that is set to 3.5 mm with 5 integration points along it. The shell offset has been configured to the middle surface.

As the model is simulated convergence issues become evident. Upon scrutinizing the warning nodes associated with contact using the ABAQUS ODB display group, the problem can be traced to a location on the bottom roller, as illustrated in Figure 2.2.2. The critical point in this context is a sharp ninety-degree corner present in the roller's sketch. To resolve this, the incorporation of a radius into the roller's geometry proved effective, successfully tackling the encountered issue at the initial station, as depicted in Figure 2.2.3.

As per the ABAQUS manual, the surface of rigid parts must be closed in order for slave nodes not to become trapped behind during contact. Three dimensional solid analytical rigid parts automatically receive a closed surface, however they can still have sharp corners which, if possible, ought to be better defined with a fillet to avoid these issues [9]. Moreover, it's important to state that the curved surfaces along the radius of analytical rigid parts will always be simulated with the same number of segments regardless of their radius, which might result in surfaces that are not sufficiently smooth for certain applications.

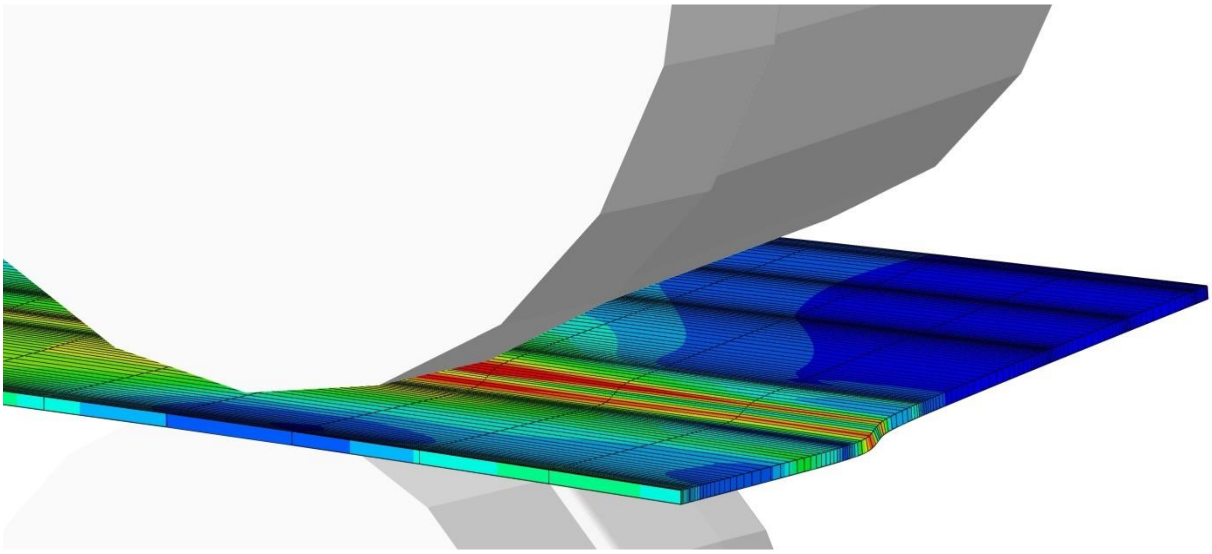

Figure 2.2.2: Location of convergence issue of bottom roller

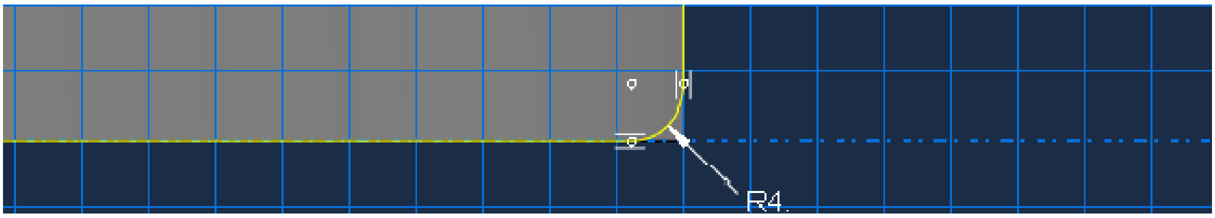

Figure 2.2.3: Bottom Roller 4mm Fillet

In the subsequent simulation, convergence problems reappeared at a later stage (Figure 2.2.4). It's crucial to highlight that the roller surface in question was already smooth at the location of the new warning node. Modifying the fillet located there would entail altering the roller geometry. In an attempt to further smooth the curvature, a segmented fillet was created to simulate a smoother curve than the standard fillet generated by ABAQUS (Figure 2.2.5). However, this adjustment did not resolve the issue, and the simulation was aborted in the same position.

To make progress, a coarser mesh was implemented, enabling the plate to advance further into the rollers successfully. However, the simulation was still aborted at a later stage due to convergence issues. Using a coarser mesh is not ideal, as it will not provide as accurate a field output in areas with higher stress. This would make it more challenging to compare data with the corresponding data of the primary simulation [10].

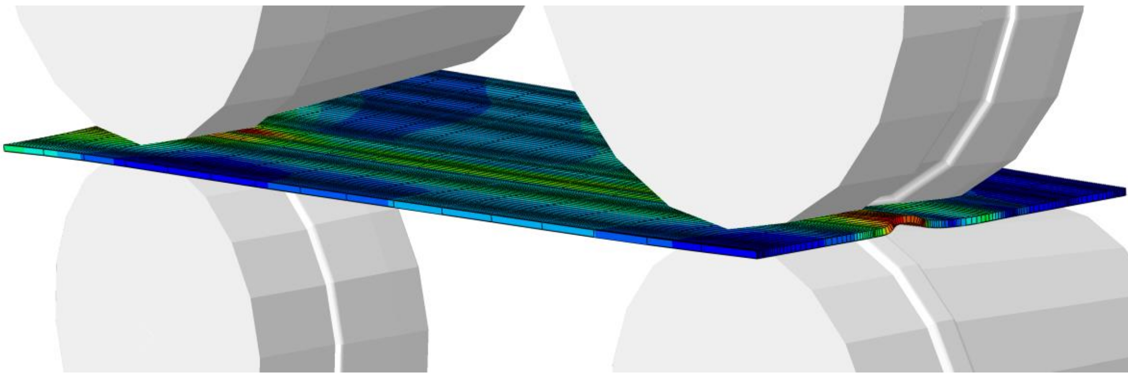

Figure 2.2.4: Second location of convergence related issues

Figure 2.2.5: Automatically and manually segmented fillet

By default, ABAQUS terminates the simulation after a maximum of five attempts to achieve convergence for a given increment. It is feasible to extend this limit to a slightly larger number, such as 10, in an attempt to attain convergence [9]. While this can be a viable solution when convergence issues are infrequent, it comes with the drawback of demanding substantial computational power for minimal gain, as each unsuccessful iteration further reduces the increment size.

This approach may be considered for shell elements to facilitate the completion of the simulation. However, the data suggested that ABAQUS demanded more increments to complete a given step when using shell elements compared to three-dimensional elements. The solver encountered challenges with converging to a solution across numerous increments, indicating a broader issue that created isolated problems in several regions. This seemed to be a general incompatibility between the mesh size, structure of shell elements and the deformations and forces they experience, compounded by the required surface-to-surface discretization contact condition.

It should be noted that contrary to node-to-surface discretization, nodes from the master surface are unable to penetrate the slave surface which renders it smoother. Although there are some options available for further smoothing, these are not beneficial when large deformations and finite sliding are expected. Furthermore, geometric curvatures that have not been defined adequately with their mesh size do not stand to benefit from the inherent smoothing of surface-to-surface discretization.

Additional efforts to use shell elements were made by utilizing discreet rigid parts. These are underformable but meshed parts which can replace analytical rigid parts. Using a finer mesh at desired roller locations their geometry can be better defined to aleviate convergence issues. While maintaining the same settings for surface interaction between the plate and the rollers, the use of discreet rigid parts enables a path-based tracking algorithm to be applied.

Nonetheless the most common issue encountered is still snagging of the plate nodes behind roller surfaces. Several locations where snagging occured could not be overcome with the introduction of a fillet radius. The issue could only be eliminated by extending the surface edge of the rollers at locations it would occur (Figure 2.2.6). This can be more taxing to compute as a slightly larger part of the plate surface is in contact with the rollers.

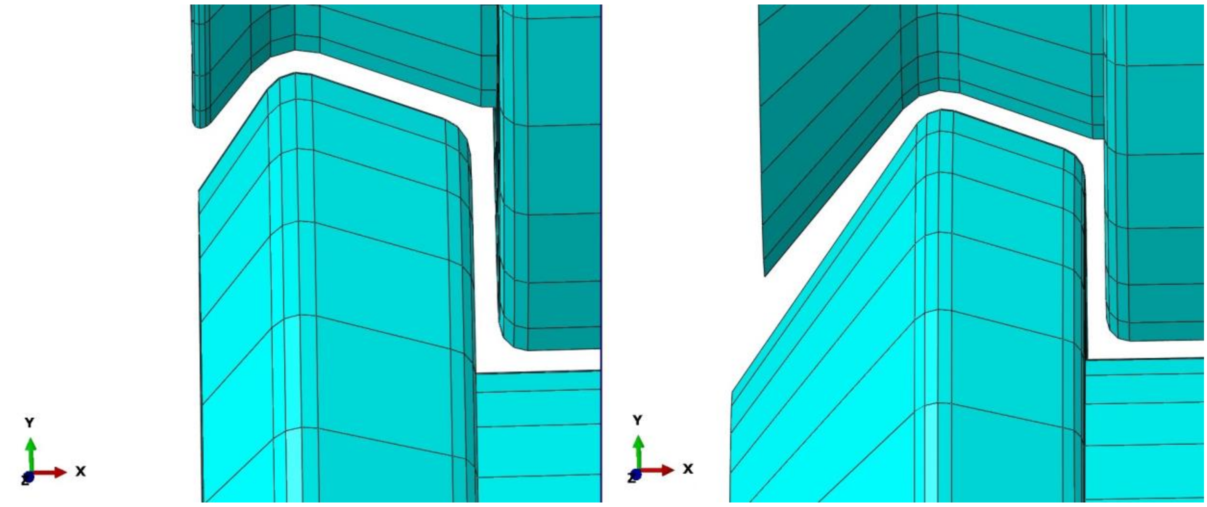

Figure 2.2.6: Roller surface extension to eliminate snagging

Even though the plate was able to advance much further with discreet rigid parts for rollers, the simulation was not completed as more convergence issues were encountered that could not be overcome (Figure 2.2.7). Depending on their mesh size discrete rigid parts can be more computationally taxing than analytical rigid parts and would thus probably not be superior based on performance encountered in this application.

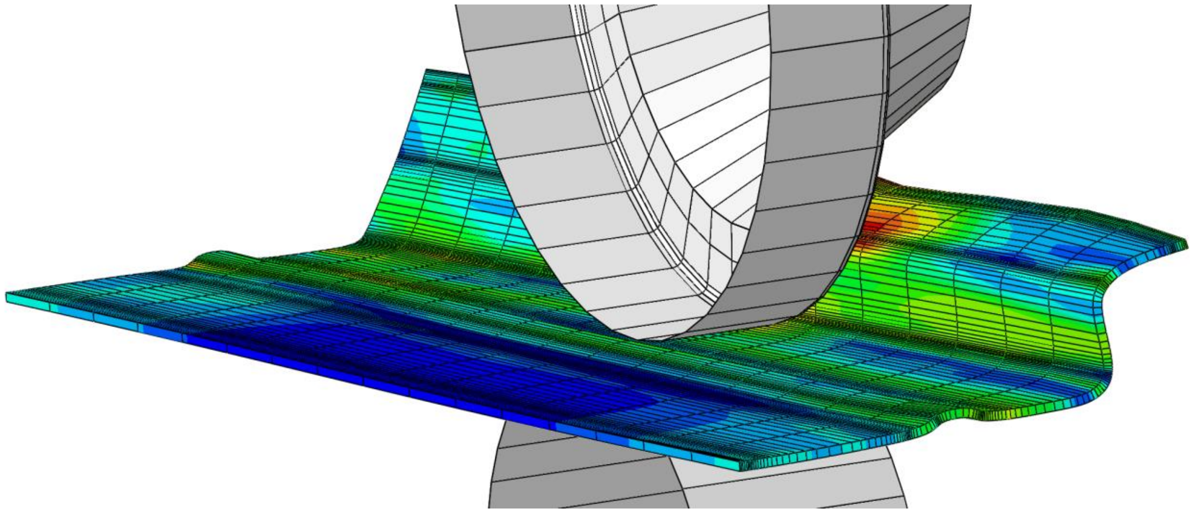

Figure 2.2.7: Ultimate point of convergence issue encountered with discreet rigid rollers

2.3 Removing Roll-Forming Stations

Corners are gradually formed during the roll-forming process, and it is optimal for this shaping to occur incrementally to minimize undesired strains and buckling phenomena in the flat faces. Plastic strain is expected to decrease when a more gradual approach with more forming stations is used as it leads to a better recovery of strains [5]. While having a large number of forming stations is ideal for achieving this gradual formation, resource constraints can make it less preferable. To control costs, simulating the roller design for a section proves to be the most effective approach. This method offers a flexible design and testing environment, regardless of certain limitations in some areas. It proves to be an essential tool, allowing easy adjustments to material characteristics and dimensions, and enabling experimentation with various roller shapes and setups. This flexibility is particularly advantageous when attempting to attain a desired curvature in the section's corners with a minimal number of stations, effectively managing undesired deformations, and reducing springback. At an industrial level, the design of rollers, their distance, and rotation speed are all parameters that are not defined by a fixed set of rules. Therefore, this process relies on experience and experimentation, and requires a significant amount of time [5].

With the goal of improving simulation time, some of the intermediate stations in the forming sequence of a corner were removed, and the gaps created in the ABAQUS assembly were eliminated after station repositioning. This process required some trial and error since removing some stations could cause interference between the plate and the preceding station. New types of plastic deformations and residual stresses which can alter the final geometry need to be minimized. Care is taken to maintain a smooth movement of the plate through the series of rollers. Splitting the simulation when using this iterative testing method can spare considerable time.

Corner two of the profile is the first one that is formed through stations one to two. Corner three is formed through stations three to eight. Being a rather simple ninety-degree bend, it is possible to remove every other station without causing interference. Similarly, the forming of corner four and five overlaps with the forming of three and four. With some experimentation, an effective combination of active stations is established without altering roller geometries significantly. Corner four's final forming happens in station thirteen instead of twelve because it shares the same ninety-degree final bend that is required for its shaping while also introducing the final bend for corner five. Figure 2.3.1 illustrates the forming sequence and how some rollers form two bends simultaneously.

The forming of corner one, which is formed last, does not overlap with previous corners. Some intermediate stations were removed while subsequent stations were left unaltered due to interference problems. The final stations, which are finishing passes, were removed entirely as, after examination, they did not influence the final geometry or stress levels significantly enough for the subsequent research.

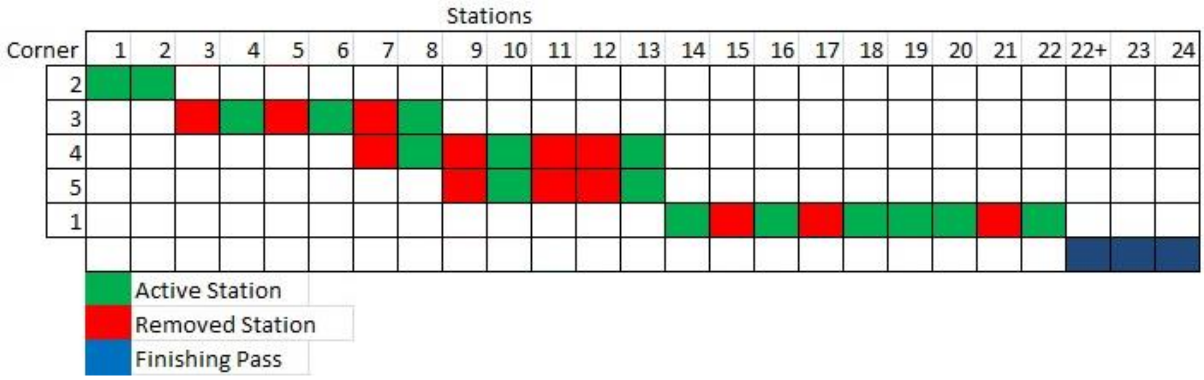

Figure 2.3.1: Forming Sequence

The resulting profile geometry (Figure 2.3.2) has no major defects except for a small deformation at the corner of the plate, which is caused at the moment the plate enters roller 13, forming corners four and five. This phenomenon can be attributed to the deactivated rollers of station 11 and 12, which help gradually form those corners. Because this deformation is only present close to the point of entry into the roller, and the plate is unaffected farther along its length, efforts to improve the shape in that area are not made.

Another phenomenon that can be observed is increased springback. After the removal of forming stations, the profile's corners are no longer formed as gradually as they were originally. As is suggested in literature, bending rate affects springback, and so this is to be expected. Corner one is the most affected and, after calculating, is revealed to be two degrees out of square.

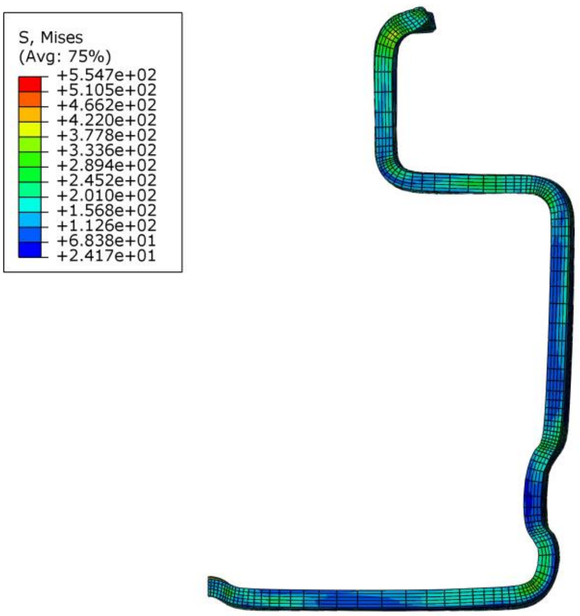

Figure 2.3.2: Resulting geometry of FEM with reduced forming stations

2.4 Splitting Of Simulation

Optimization has been performed on the model. This includes simplifying the analytical rigid roller models by adjusting their geometry to reduce the overall number of segments needed for simulation. Unnecessary interactions and boundary conditions are activated or deactivated based on the position of the plate, with activation limited to only three stations per step, excluding the entry and exit of the forming sequence.

As anticipated, ABAQUS experiences exponential slowdown as the number of stations in the simulation increases. To mitigate this issue, the simulation can be divided into segments. This disrupts the continuous material condition as the plate completely exits the rollers at the splitting point. Nonetheless, exploring the advantages and disadvantages of this method is worthwhile.

The forming sequence of the model with reduced forming stations is divided into five segments. Five copies of it are created within the same file. For each model, the relevant rollers are kept active, while the others are suppressed, and minor adjustments are made. A predefined field is used to import the deformed plate into the subsequent simulations. To facilitate this, a restart file for the last increment of the final step is necessary, achieved by selecting a restart request in step settings with an interval of 1.

After performing all simulations in sequence, a visual inspection of the final shape reveals slight springback differences between the two. The shape of the undivided model experiences more springback, resulting in a 1 mm difference in the x-direction when comparing deformed coordinates. If the entire shape is considered using symmetry, the difference becomes 2 mm (Figure 2.4.1).

This method requires less than half the simulation time of the undivided model and has potential advantages in the design of roller sequences, as it allows for geometry modifications without starting from scratch. However, it's essential to note that plate dimensions and mesh cannot be altered midway since the predefined field cannot be used in such cases. Managing a split model entails handling split files for data extraction and analysis, which is not very convenient. Lastly, since the forming process is divided, there is no continuous material feed through the rollers, impacting deformations and residual stresses in different areas. For example, the forming of corner 3, following corner 2 formation (Figure 2.3.1), remains entirely unaffected by the split. Careful selection of positions for a split point can be beneficial for minimizing such undesirable phenomena, and there is potential for enhancements in the capabilities of such a model. It is not possible to split the simulation at a point where the plate is still in contact with the rollers to avoid these issues. ABAQUS commonly encounters challenges when two entities with appropriate contact conditions are in immediate contact at the simulation's onset, unlike the smoother process observed during a restart analysis. That is why it is generally recommended to gradually bring surfaces into contact in the beginning of a simulation.

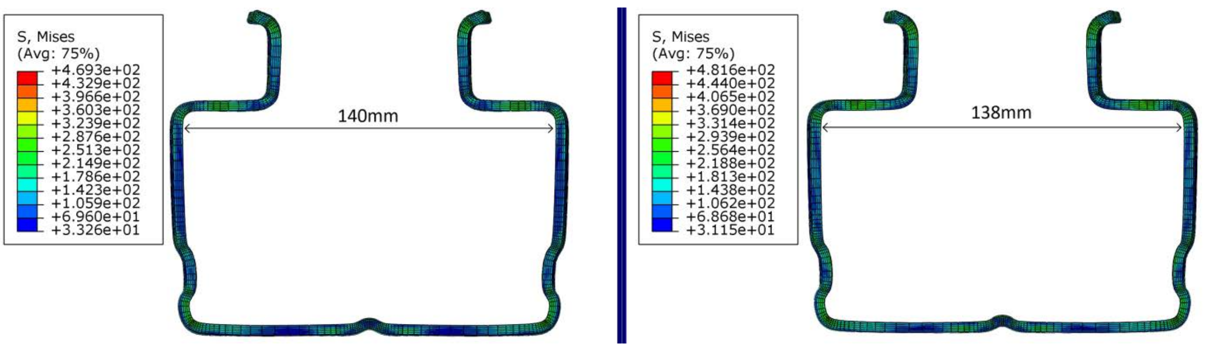

Figure 2.4.1: Undivided and split model (left to right)

2.5 Conclusions

Considering that the complete model involves 24 stations of top and bottom rollers and the issues encountered when using shell elements were at the first stations with the simplest geometry, no further research was pursued to use them successfully. Instead, further study is continued with a model that has a reduced number of forming stations, while keeping the mesh unaltered. Additionally, the material model is modified from a linear isotropic to a non-linear combined hardening model. This modification is performed because when considering cyclic plasticity phenomena, a kinematic model is required to obtain more accurate and reliable data.

Chapter 3 CYCLIC BENDING OF METAL PLATE

3.1 Hardening Parameters

A combined hardening model with two backstresses is used to simulate cyclic bending. The material retains the same density and elasticity as the original isotropic model. A suboption of cyclic hardening is selected to describe the hardening or softening behavior exhibited by the material.

Obtaining the necessary parameters for the model involves utilizing experimental hysterisis loop data aquired from material tests performed by Christos Prosgolitis. Once the stress-strain loop reaches a steady state, a stabilized cycle is derived from the data. An essential step is to shift the strain axis by the value of plastic strain at zero stress. The insertion of these values into ABAQUS generates the required hardening parameters in the input file [9]. To fine-tune these parameters single-element cyclic stress simulations can be conducted at different strain magnitudes and then compared with available experimental data. The adjustment of parameters continues until a desired level of accuracy is achieved.

It's important to note that achieving a perfect match of material behavior across an extensive range of strain values is not feasible. Therefore, it is advisable to use a set of parameters fine-tuned to closely match the strain values that are expected. In the case of the sheet metal coiling with a coil radius of 254 mm, the plastic strain magnitude reaches a maximum of 0.006 when analysing the results in ABAQUS (Figure 3.1.1).

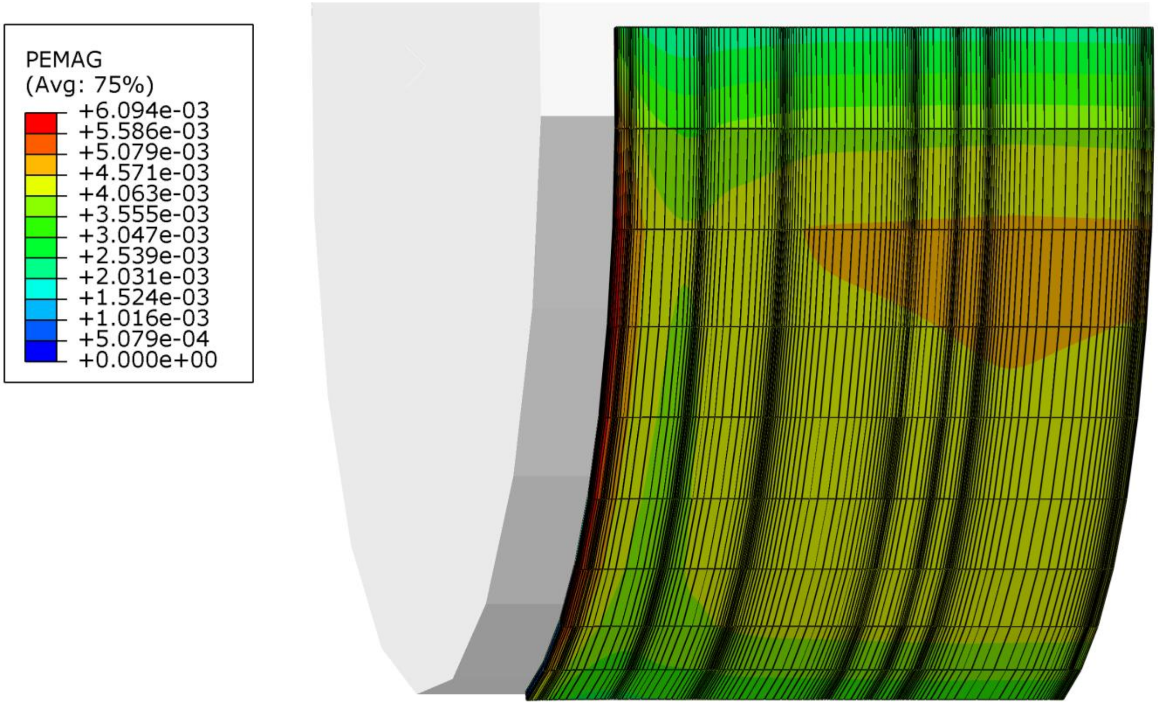

Figure 3.1.1: Plastic strain magnitude at the peak of bending with cylinder; higher stress area visible on the unconstrained left side

The linear kinematic material model is a basic representation offering an initial approximation of metal behavior under cyclic loading. Although the nonlinear isotropic/kinematic hardening model can provide a more precise outcome in numerous cyclic loading scenarios, it comes with limitations. Calibration is necessary, taking into account the expected magnitude of strain cycles relevant to the application. As per the ABAQUS documentation, the nonlinear kinematic hardening model yields significantly improved results in cyclic loading situations. However, a drawback is that it assumes uniform hardening across all strain ranges, contrary to observations in literature. Additionally, if a specimen undergoes cyclic deformations at two different strain ranges consecutively, the deformation experienced during the initial cycle influences the subsequent cycles' isotropic hardening behavior [9].

A comparison was conducted between two combined hardening material models, both describing S355MC material and incorporating the cyclic hardening option. The first model was calibrated close to the appropriate experimental cyclic stress-strain data, making it better suited for the cyclic bending simulation and the magnitude of strain expected there. The second model is fit to the monotonic stress-strain data and will be used in the roll-forming simulation with initial conditions. The yield plateau that happens because of imperfections in the crystal structure cannot be described with this model and some compromise has to be made. The results of single-element cyclic and uniaxial loading simulations clarify that the first model is not suitable for larger strains and better fits the small-strain stabilized cycle curves (Figure 3.1.2, 3.1.3). In contrast, the second model is more appropriate for larger strains and deformations.

S355MC exhibits a small amount of cyclic softening which can be observed in the cyclic stress-strain data (Figure 3.1.2). A peak difference of 10 to 20 Mpa can be observed between the first two cycles with subsequent cycles being very stable with very little change. This behaviour can be incorporated into the material in ABAQUS with the suboption for cyclic hardening which needs three parameters to be fully described. These parameters are equivalent stress which is identical to the materials yield stress at zero plastic strain, Q-infinity which is equivalent to the increase in MPa between the first and last cycle after a hypothetical infinite number of cycles, and hardening parameter b which describes the rate of increase for each cycle. Positive Q-infinity values describe hardening while negative values describe softening.

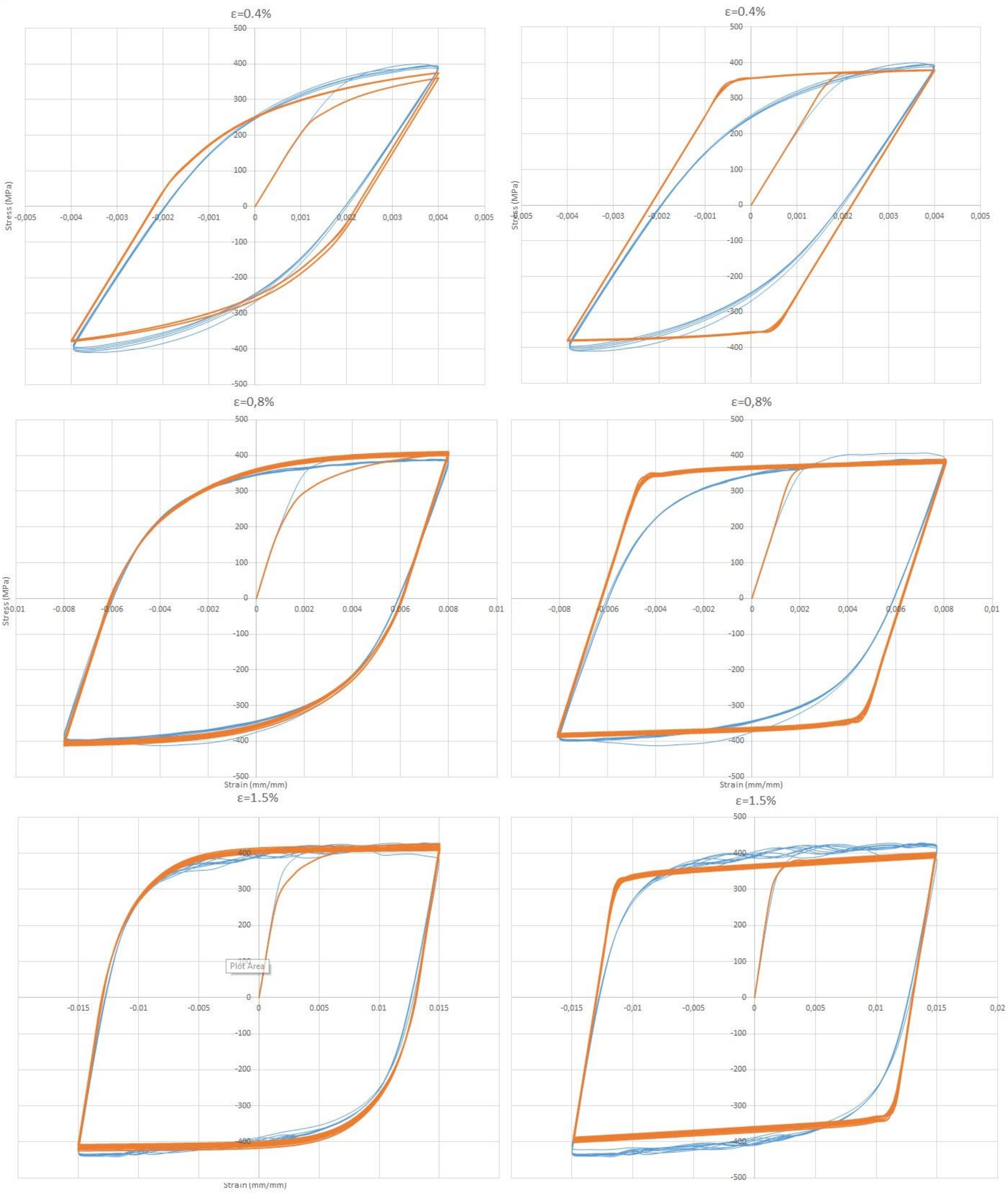

Figure 3.1.2: Curve fitting of experimental data with simulation data; left column model 1 and right column model 2

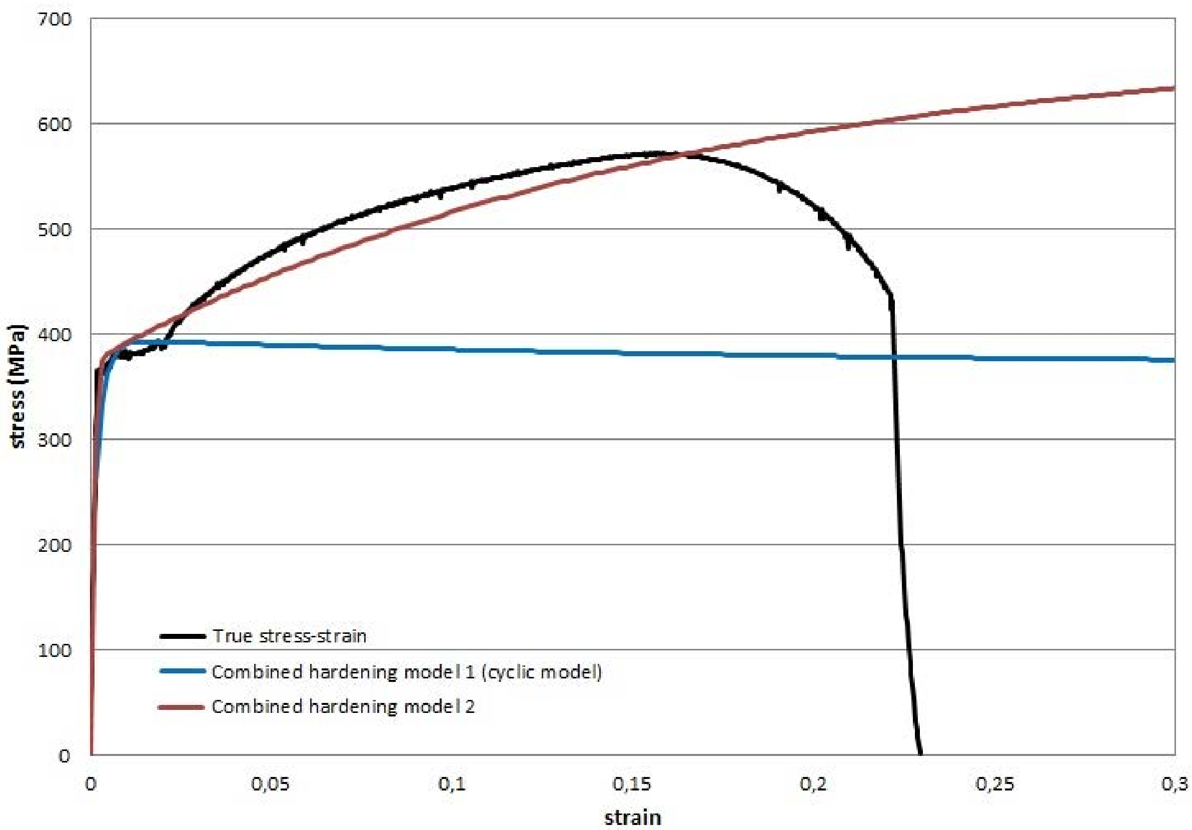

Figure 3.1.3: True stress-strain curve of experimental data and of both combined hardening models

3.2 Bending Simulation

Due to the symmetry of the plate in the roll-forming simulation, only half its width is simulated, and symmetry in the YZ plane is utilized as a boundary condition. This approach allows the plate's final state, after bending, to be used as an initial state for the roll-forming simulation, as the two plates are identical in their mesh and element structure, which is necessary for the predefined field.

Initially an extra analytical rigid part was created. A cylinder used for bending with a diameter of 508 mm which simulates a coil wide enough to cover the plates width (Figure 3.1.1). However it relied on surface interactions between the two and was significantly more demanding to complete. As a result a different approach was used that did not require these conditions.

This bending approach consists of three steps: an initial step, one involving bending, and another for the relaxation of the plate, resulting in a flat shape. To model the bending of the plate along its length to the appropriate radius, one side of it is encastred, while a rotation is applied to the opposite side. The coil diameter for transporting 3.5 mm sheet metal in the industry is 508 mm; this rotation corresponds to a theta value of 2.56 radii (Figure 3.2.1). As the material is wrapped around the radius and around itself, the radius essentially grows larger. Therefore, the smallest radius is chosen to maximize the effects of the coiling process and its subsequent impact on the roll-forming process.

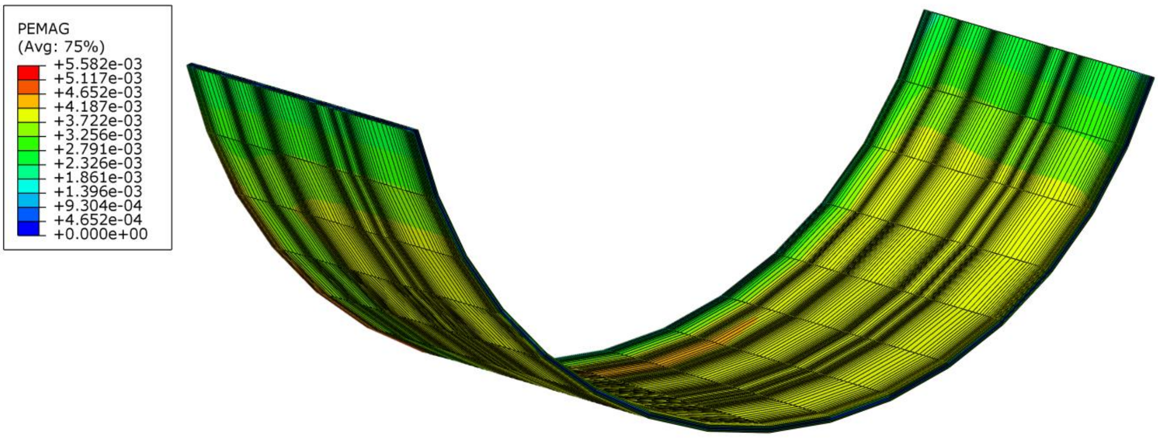

Figure 3.2.1: Plastic strain magnitude at the peak of bending

A sinusoidal amplitude in tabular form is used for the boundary condition. The negative values of the wave form are adjusted in such a way that the plate would come to rest in a flat shape if the rotation forces were to be deactivated after each cycle of bending (Figure 3.2.2). The reaction moment becomes zero for a value of theta equal to zero, indicating that the plate has reached a flat shape at that point in the simulation (Figure 3.2.3).

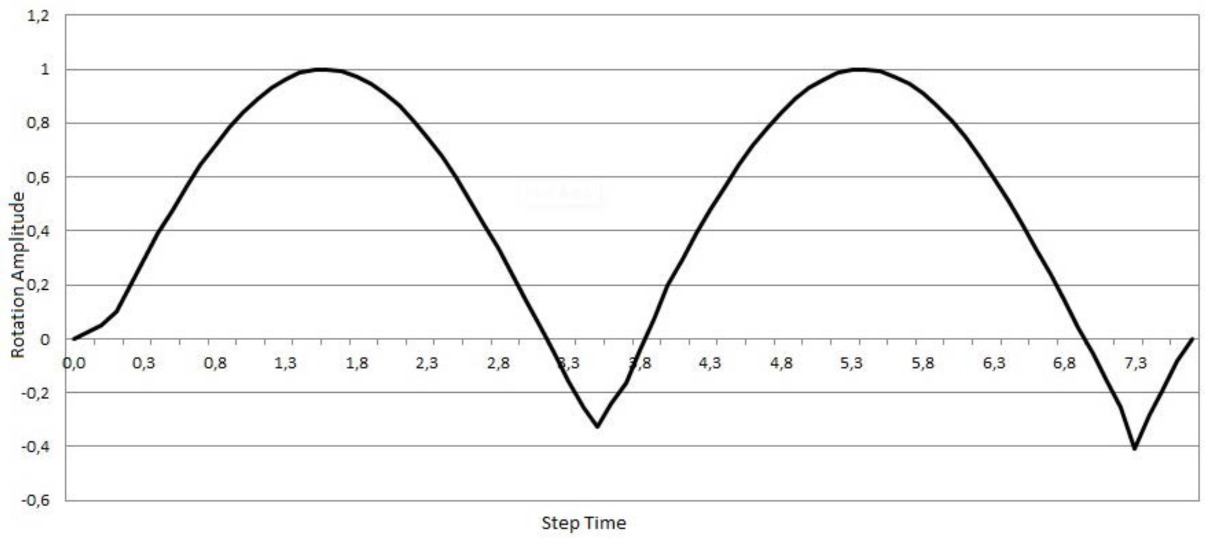

Figure 3.2.2: Rotation amplitude to step time

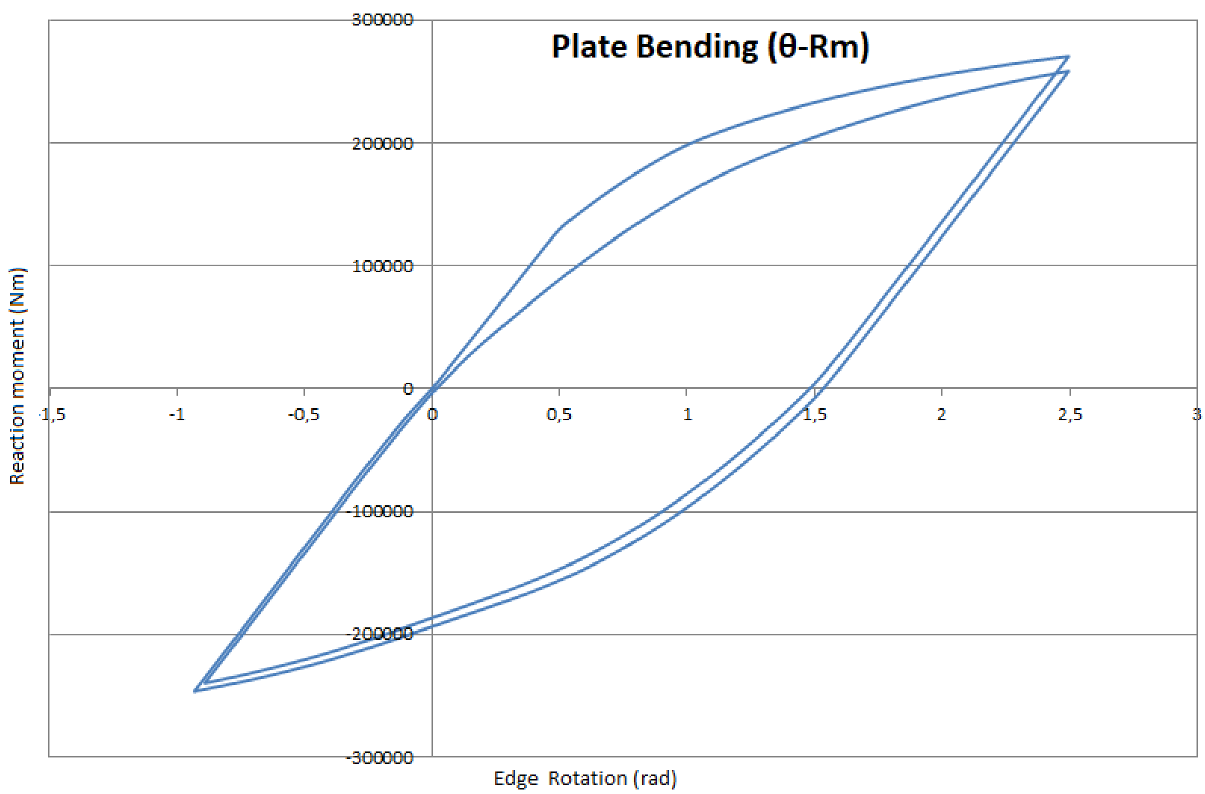

Figure 3.2.3: Rotation of plates edge and reaction moment

The stress distribution on the plates surface is generally even, with the only exception being elements closer to the unconstrained side of the plate (Figure 3.1.1, 3.2.1, 3.2.4). After selecting several locations on the plate and examining the data it is revealed that the middle layer exhibits minimal residual stresses, registering zero for other values such as equivalent plastic strain and backstress tensors. This is expected, as with each bending cycle, one side of the plate is under tension while the other is under compression. This leads to a neutral plane in the middle of the plate's thickness with minimal deformations (Figure 3.2.4) suggesting that the majority of hardening will occur near the surface, away from the neutral bending axis. Table 3.2.5 displays the yield points at four locations on the plate. The middle layer of elements exhibits no change in yield strength as it has received minimal deformation. Other layers show a decrease in yield strength which can be attributed to material softening as described by the model in Chapter 3.1. It might have been expected for both outside layers to exhibit the biggest increase as these will be subjected to the largest forces and plastic strains, however given the unique nature of bending the sheet metal on one of its sides (Figure 3.2.2) in combination with cyclic softening, subsequent plastic strain will raise the yield point of the material, resulting in these values. Additionally, if we consider the entire strain history using equivalent plastic strain values (Figure 3.2.4) it can be expected for strain hardening to occur.

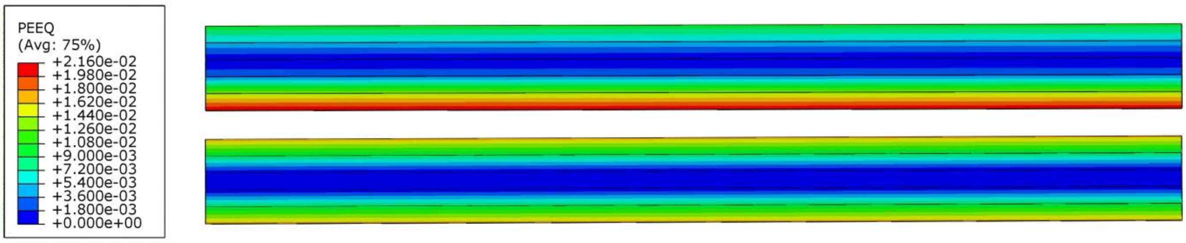

Figure 3.2.4: Neutral bending planes of unconstrained and constrained sides after bending

Table 3.2.5: Yield points across the thickness at four different locations on the plate

Layer	Position 1	Position 2	Position 3	Position 4
5	385	386	384	384
4	355	365	352	365
3	365	365	365	365
2	378	374	373	375
1	362	370	361	372

Chapter 4 ROLL-FORMING WITH INITIAL CONDITIONS

4.1 Predefined Field

In this chapter, the plate that has undergone bending will now be subjected to roll-forming using the model with a reduced number of forming stations. It is beneficial to have separate models for bending and roll-forming as this approach is economical in terms of computation time and also enables separate modification for each model. For example, different configurations of bending cycles can be tested with greater ease but material and element mesh or type would still need to be altered on both models to satisfy the predefined field conditions.

The final state of the metal plate, post bending, is transferred to the original roll-forming simulation using a predefined field. This establishes an initial state that imports element data from the final frame of the bending simulation, utilizing the same step settings as when splitting the analysis in Chapter 2.4. The plate commences the simulation with all the stresses and equivalent plastic strains induced by the bending process (Figure 4.1.1). This includes the shape, which has become slightly deformed and is marginally curved (Figure 4.1.2). A deflection of 5.18 mm can be calculated at the far end using the deformed element coordinates in ABAQUS. As the plate is 650 mm in length, this curvature is insignificant enough and will not interfere with subsequent forming and its passing through the rollers.

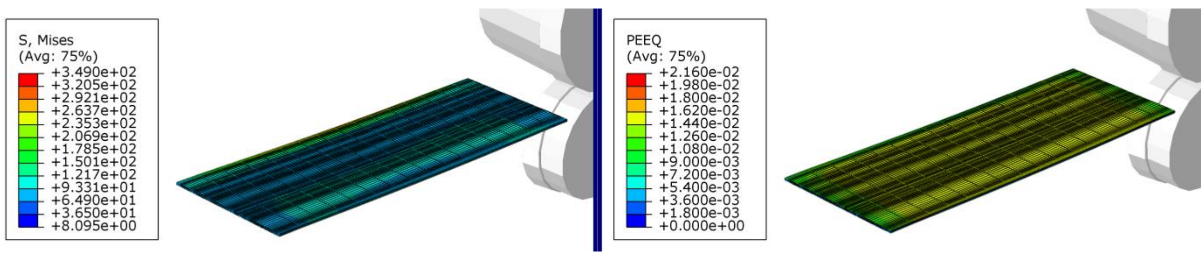

Figure 4.1.1: S,Mises and PEEQ at the start of the forming sequence

Figure 4.1.2: Sheet metal plate after being subjected to two cycles of bending; seen from the side with perspective view deactivated (straight line for visual aid)

It's crucial to highlight that the plate's hardened state is also transferred through backstress tensor data using the predefined field [9]. Although the material currently employed is the second model (Figure 3.1.3), better capable of accurately describing larger material deformations, it maintains the same cyclic hardening parameters, with the only distinction being a slightly higher yield point. A slighlty lower than the nominal yield point was necessary for the first model to align the curves of small strain cyclic loading (Figure 3.1.2). Cyclic hardening is a sub-option and should not be confused with the necessary plasticity parameters for the nonlinear combined hardening model of the material.

Using the same roll-forming model and a pristine plate with no load history, it is possible to acquire a section to use as a base for data comparison. Analyzing the shapes obtained from both simulations, no noticeable distinctions are immediately evident. Examining the displacement data to obtain the final coordinates of the element nodes and calculating approriate distances it is possible to acquire an accurate measurement. As anticipated, no variation is detected along the symmetry plane, while moving towards the edge of the plate along the profile, differences become more pronounced. The increased x and y values of the hardened plate suggest that the material is slightly more challenging to form compared to the plate of pristine material.

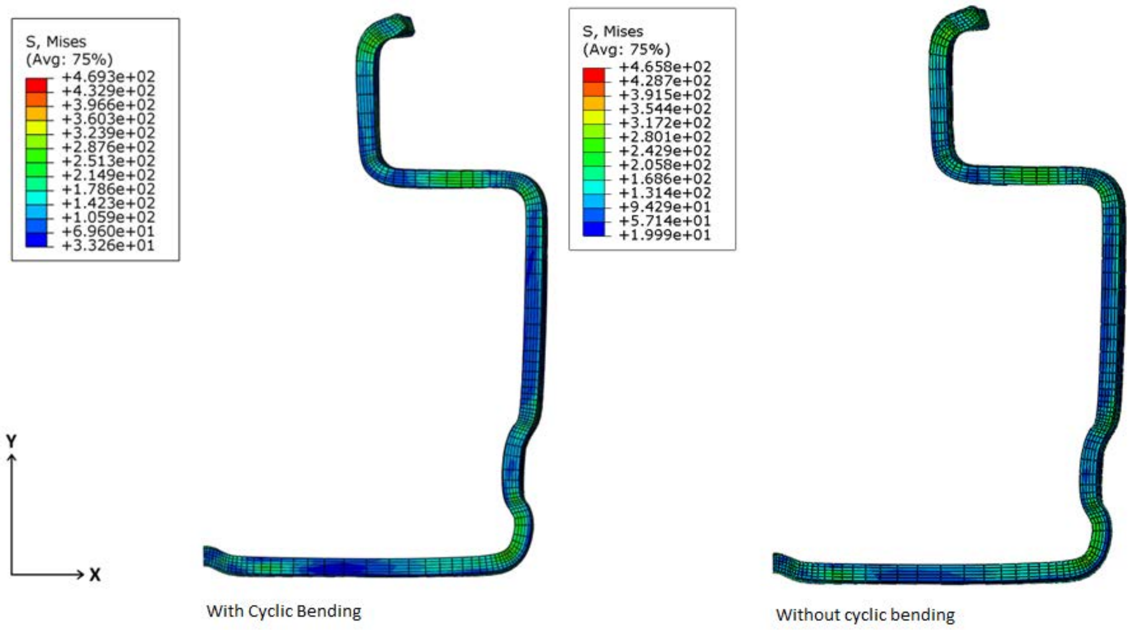

Figure 4.1.3: Final geometry of sheet metal plate with and without initial conditions.

At this point it is also necessary to compare the resulting section geometry to manufacturer tolerances (Figure 4.1.4). This reveals that corner one is largely out of square and as a result the sections width and opening is affected the most. Corner five also suffers from this and thus the sections height is also affected. Corner four is also visibly out of square albeit to a smaller extent.

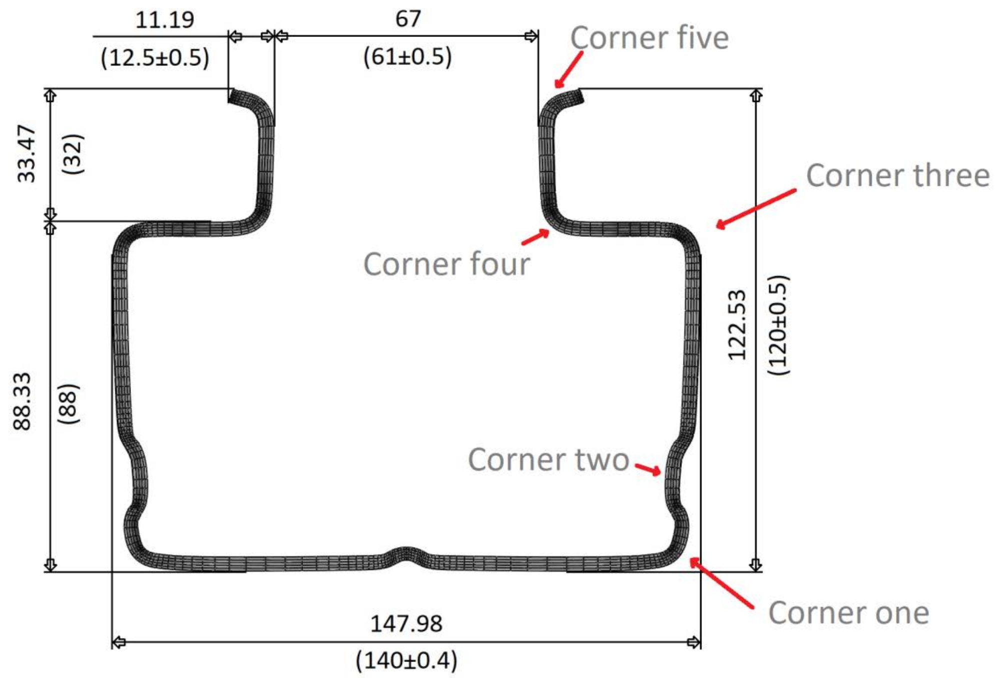

Figure 4.1.4: Dimensions of section after cyclic bending with manufacturer tolerances in parenthesis [1]; all values in millimeters

Table 4.1.4: Manufacturer and simulated plate dimensions in millimeters [1]

Manufacturer dimensions	140±0.4	120±0.5	61±0.5	12.5±0.8	32	88
Plate with cyclic bending	148.26	122.53	67	11.19	33.47	88.33
Plate without cyclic bending	147.98	121.82	66.58	11.19	33.81	88.72

These differences to the desired dimensions can be mostly attributed to the changes made to the roll-forming model. Specifically the reduction in forming stations which results in less gradual bending. As mentioned before, reducing the number of forming stations can have effects on springback and on residual stresses. However, it should also be noted that in an attempt to fit the monotonic stress-strain curve as accurately as possible, some assumptions were made regarding the curve of the kinematic material model. It is not possible to perfectly fit both the yield plateau and the hardening part of the curve that structural steels exhibit. In an attempt to approximate both to an adequate level, a higher yield point of 365 MPa is chosen rather than 355 MPa as is the nominal value of S355MC material. Subtle changes to material properties can affect the final geometry of the section.

4.2 Single Element Uniaxial Tensile Test Simulation

Using a model to simulate a uniaxial tensile test allows for an understanding of the strength enhancements resulting from roll-forming. Elements of interest can be selected from the analysis, particularly focusing on high-stress corner areas.

This finite element model comprises a single element with the same material as the forming simulation, identified as model 2 (Figure 3.1.3). One of its faces is restrained with boundary conditions, and a suitable load or displacement is applied to the opposite face. Poisson phenomena are considered by leaving the relevant degrees of freedom unrestricted on the element face that has been pinned.

Once again, a predefined field can be employed to infuse the element with the correct data from the final increment of the last step. This time, two predefined fields are necessary because only a single element is used rather than an entire mesh. One for the stress data and one for the hardening data, which includes equivalent plastic strain and all the backstress tensor data for hardening.

After the initial step in which the predefined fields are created, a second step is necessary to enable the dissipation of residual stresses. Without this relaxation step, the stresses would interfere with the tensile test, dissipating concurrently with the loading. Consequently, the loading occurs in a separate third step.

This procedure is executed on a strip of elements along the width of the plate and on each of the five layers (Figure 4.2.1). A central part of the plate is utilized to mitigate phenomena induced by the plate entering or exiting the rollers. The large amount of data is handled with various user subroutines and the resulting yield points can be visually interpreted by generating a diagram of yield stress to element position for each layer.

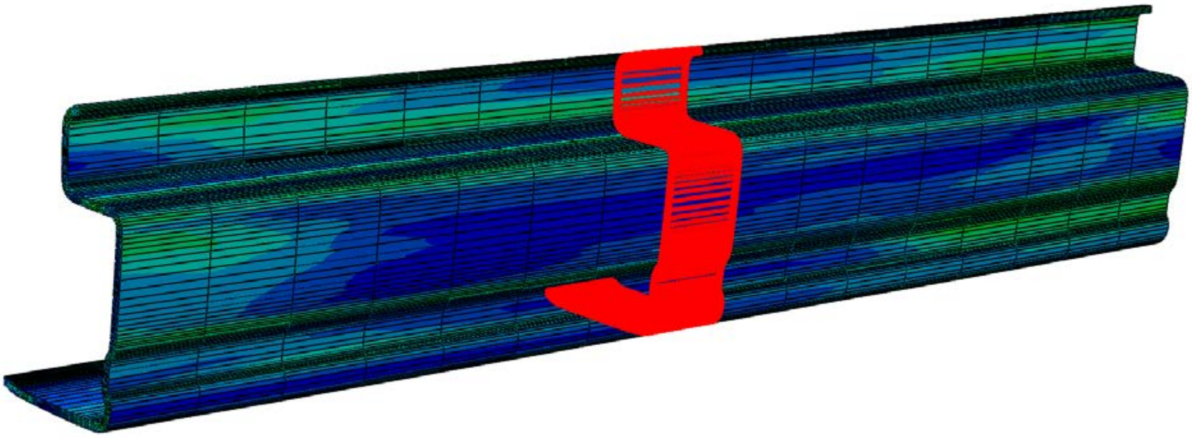

Figure 4.2.1: Element region on which yield stress analysis is performed

Initial observations can be made for yield stress behavior by analysing elements along corner three. The inner and outer layers, constituting the surface, exhibit the most significant yield stress increase.Their values near the corner apex are very close, while higher in the inner layer as the element distance from the apex increases. The middle layer demonstrates the least increase, whereas elements in layer two exhibit a higher yield point than layer four near either side of the apex.

Figure 4.2.2: Yield stress distribution across corner 3

For an understanding of how plate bending affected the results of roll-forming, the above mentioned results are then compared with data from a simulation involving a plate of pristine material. Single-element tensile tests can be conducted on the same elements to analyze their respective yield points.

The external layers reveal the most significant differences (Figure 4.2.3). Elements near the apex of the corner do not display substantial stress increase compared to those positioned further away, nearer to the sides' flats. This particular increase can be fully attributed to the bending perfomed before roll-forming. Layer 2 appears to be an exception as the hardened material has a lower yield point in the flat regions. This can be explained with the results of Table 3.2.5 which indicate that this layer experienced a particular amount of strain that left it in a softened state after cyclic phenomena. While the other layers experienced more strain and after initial cyclic softening, strain hardening caused a greater increase. This phenomenon can be attributed to the way in which the plate was bent (Figure 3.2.2) .

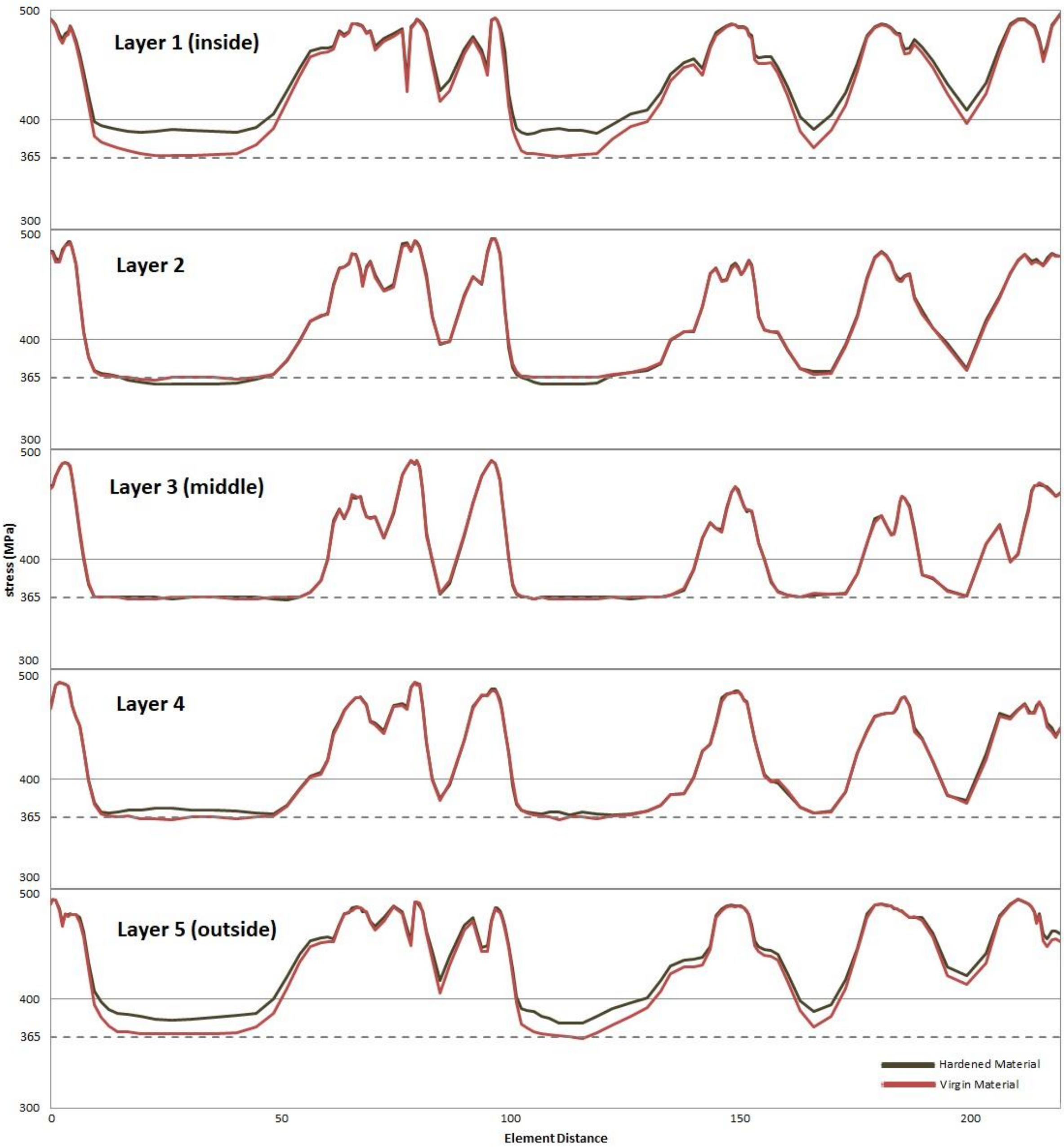

Figure 4.2.3: Yield stress graph of hardened material with two cycles of bending and virgin material

During the process of roll-forming, there might be a notable improvement in the flat faces. This is because the longitudinal forces experienced during the forming process can be relatively high, potentially causing plastic straining and contributing to gains in these areas [10]. However, the plate of pristine material exhibits little to none such increase that could be attributed to this phenomenon.

This analysis is also performed on a plate with only one cycle of bending (Figure 4.2.4). Results are similar, with the increase in yield stress of the hardened plate being smaller.

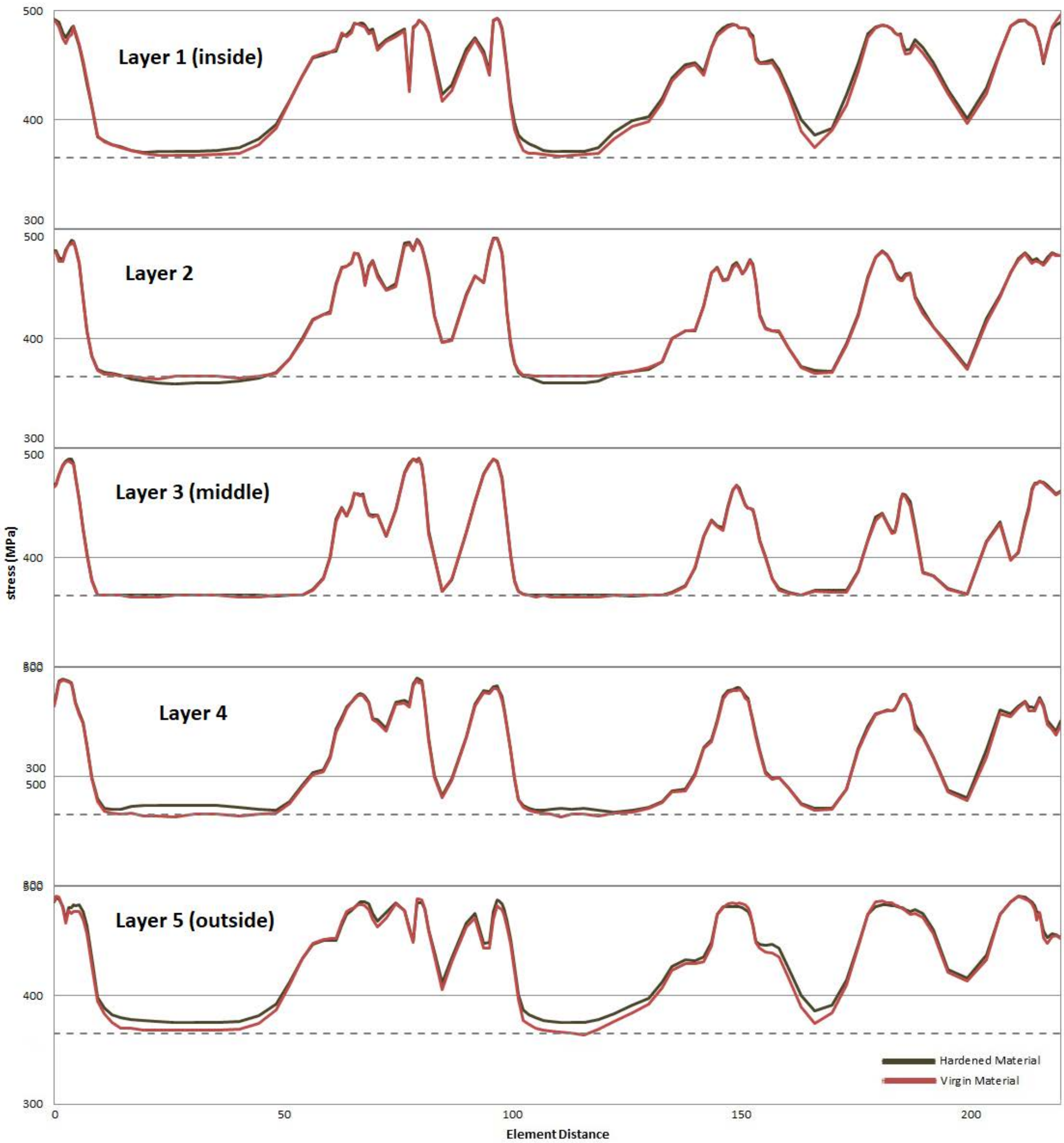

Figure 4.2.4: Yield stress graph of hardened material with one cycle of bending and virgin material

Chapter 5 CONCLUSIONS - SUGGESTIONS FOR FURTHER STUDY

Upon reviewing the findings from the preceding chapters, it becomes evident that the folding regions of roll-formed metal parts exhibit an increase in yield strength due to substantial strain hardening during the forming process. This is in stark contrast to material from the flat areas. However, when attempting to assess the impact of sheet metal coiling on material characteristics, acquiring accurate data to illustrate these effects can prove challenging. This difficulty arises from accurately describing material behavior when integrating smaller scale cyclic phenomena with large scale deformations. The results of this study indicate that an increase in yield strength is predominantly observed in the flat regions rather than the folding regions.

Calibrating kinematic hardening and cyclic hardening parameters close to the expected strain values is essential, as they fail to accurately depict larger scale phenomena without appropriate adjustments. Consequently, the introduction of a second material model is deemed necessary for the scope of this study. Despite evidence indicating increased strength in the material resulting from bending, the magnitude of this increase is relatively modest, especially when taking into account that better than ideal conditions have been considered as two cycles of bending are more than what is expected under normal industrial circumstances.

To enhance accuracy in describing material behavior across small strain cyclic phenomena to large scale deformations, potential improvements to material parameters are worth exploring. However, it's essential to acknowledge limitations associated with simulating materials under these conditions.

The roll-forming sequence can also be deemed worthy of further study, with the possibility of altering geometries to achieve sections closer to manufacturer dimensions. Careful consideration of material properties is crucial in this context. Also noteworthy is the fact that the part of the plate that comes in contact with the rollers initially, undergoes undesired deformations, only allowing the sections shape to reach a steady dimensional state further along its length. This length is influenced by the gradualness of forming and the number of stations used in the simulation. While this phenomenon cannot be entirely eliminated, its impact can be minimized through the careful selection and modification of rollers.

The resulting sections are promising candidates for loading simulations, allowing for analysis of ultimate load-bearing capacities. Buckling simulations can be conducted on the sections that have been subjected to bending as well as those that have not.

It is also crucial to emphasize that while there may be positive effects on structural integrity, especially regarding strength enhancements in profiles due to higher residual stress regions, there are also potential drawbacks. Factors such fatigue must be carefully considered for certain applications.

REFERENCES

[1] FAtigue STrength of COLD-formed structural steel details [https://fastcold-rfcs.com/] Accessed on 30.1.2021

[2] Karren KW. Corner properties of cold-formed steel shapes. Journal of the Structural Division—ASCE 1967;93:401–32.

[3] S. Afshan, B. Rossi, L. Gardner, Strength enhancements in cold-formed structural sections — Part I: Material testing. Journal of Constructional Steel Research 83 (2013) 177–188.

[4] B. Rossi, S. Afshan, L. Gardner, Strength enhancements in cold-formed structural sections — Part II: Predictive models. Journal of Constructional Steel Research 83 (2013) 189–196.

[5] Barbara Rossi , Herve Degee, Frederic Pascon, Enhanced mechanical properties after cold process of fabrication of non-linear metallic profiles. Thin-Walled Structures 47 (2009) 1575–1589.

[6] Feiliang Wang, Jian Yang, Iftikhar Azim, Li Baι, Yanling Ma, Experimental and numerical evaluations of the distribution and effect of roll-forming residual stress on CFS sigma beams. Journal of Constructional Steel Research 167 (2020) 105978.

[7] B.W. Schafer, Z. Li, C.D. Moen. Computational modeling of cold-formed steel. Thin-Walled Structures 48 (2010) 752–762

[8] Q.V. Bui, J.P. Ponthot, Numerical simulation of cold roll-forming processes. J. Mater. Process. Technol. 202 (2008) 275–282.

[9] Abaqus 6.13. Analysis User's Manual, Dassault Systèmes. Simulia Corp, Providence, RI, USA 2013.

[10] Barbara Rossi, Hervé Degée, Romain Boman, Numerical simulation of the roll forming of thin-walled sections and evaluation of corner strength enhancement. Finite Elements in Analysis and Design 72 (2013) 13–20.